

# Full- versus Sub-Regional Quantification of Amyloid-Beta Load on Mouse Brain Sections

Yuu Ohno<sup>1</sup>, Riley Murphy<sup>2</sup>, Matthew Choi<sup>3</sup>, Weijun Ou<sup>4</sup>, Rachita K. Sumbria<sup>4,5</sup>

<sup>1</sup> Henry E. Riggs School of Applied Life Sciences, Keck Graduate Institute <sup>2</sup> Crean College of Health and Behavioral Sciences, Chapman University <sup>3</sup> Keck Science Department, Claremont McKenna College <sup>4</sup> Department of Biomedical and Pharmaceutical Sciences, School of Pharmacy, Chapman University <sup>5</sup> Department of Neurology, University of California, Irvine

## Corresponding Author

Rachita K. Sumbria

sumbria@chapman.edu

## Citation

Ohno, Y., Murphy, R., Choi, M., Ou, W., Sumbria, R.K. Full- versus Sub-Regional Quantification of Amyloid-Beta Load on Mouse Brain Sections. *J. Vis. Exp.* (183), e63669, doi:10.3791/63669 (2022).

## Date Published

May 19, 2022

## DOI

10.3791/63669

## URL

jove.com/video/63669

## Abstract

Extracellular accumulation of amyloid-beta ( $A\beta$ ) plaques is one of the major pathological hallmarks of Alzheimer's disease (AD), and is the target of the only FDA-approved disease-modifying treatment for AD. Accordingly, the use of transgenic mouse models that overexpress the amyloid precursor protein and thereby accumulate cerebral  $A\beta$  plaques are widely used to model human AD in mice. Therefore, immunoassays, including enzyme-linked immunosorbent assay (ELISA) and immunostaining, commonly measure the  $A\beta$  load in brain tissues derived from AD transgenic mice. Though the methods for  $A\beta$  detection and quantification have been well established and documented, the impact of the size of the region of interest selected in the brain tissue on  $A\beta$  load measurements following immunostaining has not been reported. Therefore, the current protocol aimed to compare the  $A\beta$  load measurements across the full- and sub-regions of interest using an image analysis software. The steps involved in brain tissue preparation, free-floating brain section immunostaining, imaging, and quantification of  $A\beta$  load in full- versus sub-regions of interest are described using brain sections derived from 13-month-old APP/PS1 double transgenic male mice. The current protocol and the results provide valuable information about the impact of the size of the region of interest on  $A\beta$ -positive area quantification, and show a strong correlation between the  $A\beta$ -positive area obtained using the full- and sub-regions of interest analyses for brain sections derived from 13-month-old male APP/PS1 mice that show widespread  $A\beta$  deposition.

## Introduction

Alzheimer's disease (AD), the sixth leading cause of death in the United States, continues to be a public health threat, with an estimated 6.2 million Americans living with

AD. This is expected to reach 13.8 million by 2060<sup>1</sup>. To date, symptomatic management through medications such as cholinesterase inhibitors and memantine is the primary

course of treatment<sup>2</sup>. AD is characterized by neuropathologic manifestations such as extracellular deposition of amyloid-beta ( $A\beta$ ) plaques and intracellular hyperphosphorylated tau accumulation in the form of neurofibrillary tangles<sup>3,4</sup>. Formed by an endoproteolytic cleavage of the amyloid precursor protein (APP) *via* beta- and gamma-secretase,  $A\beta$  aggregates to form oligomers and fibrils, leading to neurotoxic effects<sup>5</sup>.  $A\beta$  has been hypothesized to serve a primary pathological role since the 1980s, and is the therapeutic target of the only FDA-approved disease-modifying therapy for AD<sup>6</sup>. As a result, transgenic AD mouse models harboring mutations in genes resulting in robust cerebral  $A\beta$  accumulation have been widely used for preclinical AD research since the early 1990s<sup>7</sup>.

Detection of  $A\beta$  species in these AD transgenic mouse brains is generally done using two immunoassays: enzyme-linked immunosorbent assay (ELISA) and immunostaining. The former assay enables quantitative determination of different  $A\beta$  species and is less time-consuming compared to immunostaining, which requires several sequential tissue processing and imaging steps, including tissue sectioning, immunostaining, imaging, and quantification<sup>8</sup>. Further, the results obtained following immunostaining are semi-quantitative<sup>8</sup>. However, the ability to spatially localize  $A\beta$  makes immunostaining an attractive approach for  $A\beta$  detection in brain tissues<sup>8</sup>.

While using  $A\beta$  immunostaining, several different quantification paradigms have been employed by different research groups. For example, some research groups quantify the  $A\beta$  load in the entire region of interest (cortex or hippocampus), while others quantify the  $A\beta$  load in a specified sub-region of interest (a part of the cortex or the hippocampus)<sup>9,10,11</sup>. Though the methods for  $A\beta$

detection and quantification have been well established and documented, the impact of the size of the region of interest on  $A\beta$  load measurements following immunostaining has not been reported. Therefore, the current protocol aimed to compare the  $A\beta$  load measurements across the full- and sub-regions of interest using an image analysis software, ImageJ.

The current study used 13-month-old APP/PS1 double transgenic male mice, which express a chimeric mouse/human APP and a mutant presenilin 1, to model early-onset of AD<sup>12</sup>.  $A\beta$  deposits start developing by 6-7 months of age, and abundant  $A\beta$  accumulation is observed both in the cortex and the hippocampus of these mice by 9-10 months of age<sup>12</sup>. The transgenic amyloid peptides and holoprotein can be detected by 6E10-immunostaining<sup>13</sup>, making it a desirable animal model for the present protocol. The procedure covered herein includes brain tissue preparation, immunostaining of free-floating sections, imaging, and quantification of  $A\beta$  load in full-versus sub-regions of interest. The analysis shows a strong correlation between the full- and sub-regional quantification, indicating robust agreement between these two methods in the brain tissue sections derived from 13-month-old APP/PS1 male mice that show abundant  $A\beta$  deposits.

## Protocol

All animal experiments were conducted in compliance with the University Laboratory Animal Resources under protocols approved by the University of California, Irvine, Institutional Animal Care and Use Committee. The experiments were performed with male B6C3-Tg(APP<sup>swe</sup>, PSEN1<sup>dE9</sup>)85Dbo/Mmjax (APP/PS1) mice (13-month-old, n = 35). The mice were obtained from commercial sources (see **Table of Materials**).

## 1. Brain tissue preparation

1. Anesthetize the mice using a lethal dose of a phenytoin/pentobarbital-based anesthetic (150 mg/kg) injected intraperitoneally (see **Table of Materials**) following approved animal protocols. Perform cardiac perfusion with ice-cold phosphate-buffered saline (1x PBS) for 5 min at a speed of 5 mL/min to clear the brain vasculature<sup>14</sup>.
2. Harvest brain tissue following the previously published report<sup>15</sup>, separate into the left and right brain hemisphere and place the right hemi-brain of each mouse into a 15 mL conical tube containing 5 mL of freshly prepared 4% paraformaldehyde (PFA) solution in 1x PBS for 72 h at 4 °C.  
**NOTE:** The brains may be immersion-fixed from 24-72 h depending on the antigen being studied. The left hemi-brain, without the cerebellum, can be snap-frozen in liquid nitrogen and then stored at -80 °C, followed by processing for biochemical assays such as ELISA and biochemical A $\beta$  detection<sup>16</sup>.  
**CAUTION:** PFA is a probable carcinogen, and skin contact with PFA may lead to allergic skin symptoms. Use nitrile or butyl gloves, masks, and eye protection for handling it, and prepare under a chemical fume hood.
3. After incubation in 4% PFA, incubate the hemi-brains sequentially in 5 mL of 10%, 20%, and 30% sucrose solutions prepared in 1x PBS for 24 h, each at 4 °C until the brain tissue sinks to the bottom of the conical tube.
4. After incubation in the 30% sucrose solution, remove the hemi-brain, gently dab the brain on a filter paper to remove the excess sucrose solution, and freeze the fixed hemi-brain in powdered dry ice for 30 min. Store the

frozen hemi-brain in well-labeled aluminum foils at -80 °C until cryosectioning.

**NOTE:** In the current protocol, the hemi-brains were stored at -80 °C for 6-8 months.

5. Section the frozen hemi-brain into 20  $\mu$ m thick sections using a cryostat (see **Table of Materials**).

**NOTE:** For the current protocol, the hemi-brains were sectioned into sagittal sections, and if needed, coronal sections can also be prepared<sup>17</sup>. Step 2 is for A $\beta$  immunofluorescent staining on fixed and cryoprotected brain tissue samples.

## 2. Immunofluorescence

1. Place the sagittal brain tissue sections (step 1.5) into a 24-well plate (up to six mouse brain sections per 300  $\mu$ L per well). Wash for 5 min with 1x PBS three times at room temperature (23 °C) by placing the plate on a shaker with gentle swirling.
2. Incubate the brain tissue sections with 70% formic acid in dH<sub>2</sub>O at room temperature for 10 min.  
**CAUTION:** Formic acid is corrosive, so avoid skin and eye contact.
3. Wash the brain tissue sections for 5 min with dH<sub>2</sub>O three times at room temperature.
4. Block non-specific binding with 0.5% bovine serum albumin (BSA) and 0.3% TritonX 100 (see **Table of Materials**) in 1x PBS at room temperature for 1 h.
5. Incubate the brain tissue sections with a fluorophore-labeled primary antibody (6E10, see **Table of Materials**) diluted (1:1000) in 1x PBS containing 0.3% TritonX 100 at 4 °C for 24 h.

**NOTE:** Since the primary antibody is fluorophore-conjugated, the plate needs to be covered from this step

onward, or all work must be done in a dark room to maintain fluorophore effectiveness.

6. Wash the brain tissue sections for 10 min with 1x PBS three times at room temperature.
7. Mount the brain tissue sections onto positively-charged glass slides (see **Table of Materials**) that are well labeled (label information on the slide is based on preference), after a brief wash with dH<sub>2</sub>O to remove remaining salts. Let the slides air dry in the dark.
8. Mount the brain tissue sections with an aqueous mounting media (see **Table of Materials**) and place the glass coverslip over the tissue. Seal the ends of the coverslip with clear nail polish and store the slides in a slide box at 4 °C until imaging.

**NOTE:** In the current protocol, the slides were imaged within 1 month after staining.

### 3. Imaging

1. Image the 6E10-stained brain sections using a fluorescence (epifluorescence or confocal) microscope (see **Table of Materials**), that has a 2x objective to capture the entire brain tissue section in one image and is equipped with the appropriate filter (GFP in this work).
2. Save the captured images as a TIFF file or as required and open them in the image analysis software (see **Table**

**NOTE:** Imaging settings must be consistent across different slides.

**of Materials**) as described in step 4.2 below for 6E10 quantification.

**NOTE:** Include a scale bar before capturing the image to quantify in the image analysis software, ImageJ.

### 4. Full-region of interest analysis

**NOTE:** The present work's two regions of interest are the hippocampus and the iso-cortex. Full-region of interest analysis represents the analysis of the entire iso-cortex (referred to as the cortex going forward) or the hippocampus in the imaged brain tissue section.

1. Download the image analysis software (see **Table of Materials**) and start the software once installed.
2. Once the software runs, click on **File | Open | Choose the image** to be analyzed.
3. Click on **Analyze | Set scale | Click to remove scale**. Select the **Straight** tool from the software tool bar and draw a straight line along the length of the scale bar. Click on **Analyze | Measure**. Note the length or distance of the scale bar in pixels. Click on **Analyze | Set scale**.
  1. In the pop-up window, enter the distance in pixels, the known distance of the scale bar (in  $\mu\text{m}$  in this case), and the unit of length as  $\mu\text{m}$ . Check **Global** to apply the new scale setting to all following images if multiple images are processed. Click **OK** to apply the settings.

**NOTE:** It is always recommended to check if the accurate scale is applied to the image before further analysis.
4. To set the desired measurement to the area of the section, go to **Analyze | Set measurements | Select the Area and Display Label boxes**. Check that the image being analyzed is selected under **Redirect to**.

5. For ease of hippocampus or cortex visualization, go to **Image | Adjust | Brightness/Contrast**. Drag the **Maximum** slide bar gradually to the left to increase tissue clarity until the brain regions of interest are identifiable.  
**NOTE:** Do not apply this setting to avoid false measurements during analysis, instead proceed to the next step.
6. Use the **Polygon selection** or **Freehand selection** tool to outline the hippocampus region. Click on the **Reset** option of the **Brightness/Contrast** settings once the hippocampus is outlined to revert to the original brightness.  
**NOTE:** The steps must be repeated separately for the cortical region.
7. To measure the total tissue area of the selected region, click on **Edit | Clear outside**. Once the selected region is the only image on-screen, click on **Analyze | Measure** to obtain the **total tissue area** analyzed in a pop-up window. Save the data in an Excel file for later use.
8. To measure the 6E10-positive area, go to **Image | Adjust | Color threshold**. A pre-made filter under the **Thresholding method** usually provides desired results highlighting the strongest signals in red.  
**NOTE:** The optimal threshold selection will depend on the background of the image and the staining intensity. Select a threshold setting that picks up the stain and not the background.
9. After selecting the appropriate threshold, check **Dark background**. This will highlight the A $\beta$  spots (the stain of interest) on a black background. Click on **Select | Original | Select**, giving the dark signals (the A $\beta$  deposits) on a white background. Click on **Analyze |**

**Analyze particles** and click **OK** when the pop-up window generates.

10. Copy the summary output generated by the software by clicking on **Edit | Copy**. Paste into the previously started Excel file with respective labels. This is the 6E10-positive area in the selected regions of interest (either hippocampus or cortex).  
**NOTE:** In Excel, there will be a column for the total 6E10-positive area (step 4.10) and the total tissue area (step 4.7).
11. Calculate the 6E10-positive area (%) as follows<sup>16</sup>: (Total 6E10-positive area/Total tissue area analyzed) x 100.

## 5. Sub-region of interest analysis

**NOTE:** Sub-region of interest analysis represents the analysis of a part of the cortex or the hippocampus in the imaged brain tissue section.

1. Download the image analysis software and start the software once installed.
2. Once the software runs, click on **File | Open | Choose the image** to be analyzed.
3. Click on **Analyze | Set scale| Click to remove scale**. Select the **Straight** tool from the software toolbar and draw a straight line along the length of the scale bar. Click on **Analyze | Measure**. Note the length or distance of the scale bar in pixels. Click on **Analyze | Set scale**.
  1. In the pop-up window, enter the distance in pixels, the known distance of the scale bar (in  $\mu\text{m}$  in this case), and enter the unit of length as  $\mu\text{m}$ . Check **Global** to apply the new scale setting to all following images if multiple images are processed. Click **OK** to apply the settings.

- NOTE:** It is always recommended to check if the accurate scale is applied to the image before further analysis.
4. To set the desired measurement to the area of the section, go to **Analyze | Set measurements | select the Area and Display Label boxes**. Check that the image being analyzed is selected under **Redirect to**.
  5. Adjust the brightness and contrast if the image is too dim and the brain regions (e.g., the hippocampus or the cortex in this case) cannot be easily identified. Use the software toolbar and click on **Image | Adjust | Brightness/Contrast** and drag the **Maximum** sliders to the left as needed to increase the tissue visibility.
 

**NOTE:** Do not apply this setting to avoid false measurements during analysis, instead proceed to the next step.
  6. Using the **Rectangle tool**, select the region of interest in the cortex or the hippocampus. Use the toolbar and click on **Edit | Selection | Specify**, changing the height and width to a pre-defined value. Adjust the box, so it is completely covered by tissue. Reset the brightness/contrast to revert to the original brightness.
 

**NOTE:** The size of the box used to select the regions of interest must be consistent for all the images. For the present analysis, the box size was either 300 pixels x 300 pixels (equivalent to 1177  $\mu\text{m}$  x 1177  $\mu\text{m}$ ) or 400 pixels x 200 pixels (equivalent to 1569  $\mu\text{m}$  x 784  $\mu\text{m}$ ).
  7. Duplicate the selected region of interest by right-clicking the box and clicking on **Duplicate**. A new window with the selected region will open. Rename the duplicated image to display the region it is located in (e.g., cortex or hippocampus).
  8. Adjust the duplicated image type by using the toolbar and clicking on **Image | Type | 8-Bit** to convert the duplicated RGB image to 8-bit to best analyze the plaques. Invert the image by clicking on **Edit | Invert**.
  9. To measure the 6E10-positive area, go to **Image | Adjust | Threshold**. A pre-defined filter under the **Thresholding method** usually provides the desired results by highlighting the strongest signals in red.
 

**NOTE:** The optimal threshold selection will depend on the background of the image and the staining intensity. Select a threshold setting that picks up the stain and not the background.
  10. After selecting the appropriate threshold, select **Apply**.
  11. To analyze the 6E10-positive area, use the toolbar and click on **Analyze | Analyze particles**, ensuring the **"Summarize Results"** is checked.
  12. Copy the **Summary** output with the **%Area** generated by the software by clicking on **Edit | Copy**. Paste into the previously started Excel file with respective labels.
  13. Repeat steps 5.3-5.12 for the different regions in the tissue. Ensure the placement of each box to outline the region of interest is consistent between each image.
 

**NOTE:** The rotation tool can be utilized if the **Rectangle toolbox** dimensions cannot fit into the specified region due to tissue curvature.
  14. To rotate the rectangle, use the toolbar and click on **Edit | Selection | Rotate** and adjust the rotation degree as needed. Duplicate the image as mentioned in step 5.7 and clear the outside by using the toolbar and clicking on **Edit | Clear outside**, which clears the 6E10 stains outside the specified rectangle. Proceed with step 5.8 described above.

## Representative Results

Here, two different methods are compared to quantify the 6E10-positive area in the hippocampus and the cortex of mouse brain tissues. The two methods are the full-region and sub-region of interest analyses (**Figure 1**). The full-region of interest analysis, as the name suggests, involves outlining the entire region of interest (in this case, either the iso-cortex or the hippocampus) to determine the 6E10-positive area (**Figure 1A,B**). The sub-region of interest analysis involves selecting a pre-defined region within the region of interest to determine the 6E10-positive area (**Figure 1C,D**). The stepwise ImageJ protocol for the two methods is shown in **Figure 2**, **Figure 3**, and **Figure 4**.

This study used three readers; two independent readers performed the sub-region of interest analysis, and the third reader performed the full-region of interest analysis. As seen in **Figure 5A,B**, there was a strong significant positive correlation ( $p < 0.0001$ ) between the 6E10-positive area reported by the two readers performing the sub-region of

interest analysis (Pearson correlation coefficient  $r = 0.97$  for the cortex and  $r = 0.96$  for the hippocampus). The 6E10-positive areas reported by the two readers for the sub-region of interest analysis were averaged, and the averaged sub-region of interest 6E10-positive area shared a strong significant positive correlation ( $p < 0.0001$ ) with the 6E10-positive area obtained using the full-region of interest analysis for both the cortex (Pearson correlation coefficient  $r = 0.96$ ; **Figure 5C**) and the hippocampus (Pearson correlation coefficient  $r = 0.95$ ; **Figure 5D**). The mean cortical- and hippocampal-6E10-positive area obtained by the full-region and sub-region of interest analyses were comparable with no significant difference, confirming the agreement between the two methods (**Figure 5E**). Further, the insoluble A $\beta$ 1-42 was measured in whole-brain homogenates in a subset of mice and the cortical (**Figure 5F**) and hippocampal (**Figure 5G**) 6E10-positive area determined by the full-region of interest analysis was significantly ( $p < 0.01$ ) correlated with insoluble A $\beta$ 1-42 load using ELISA (see **Table of Materials**).

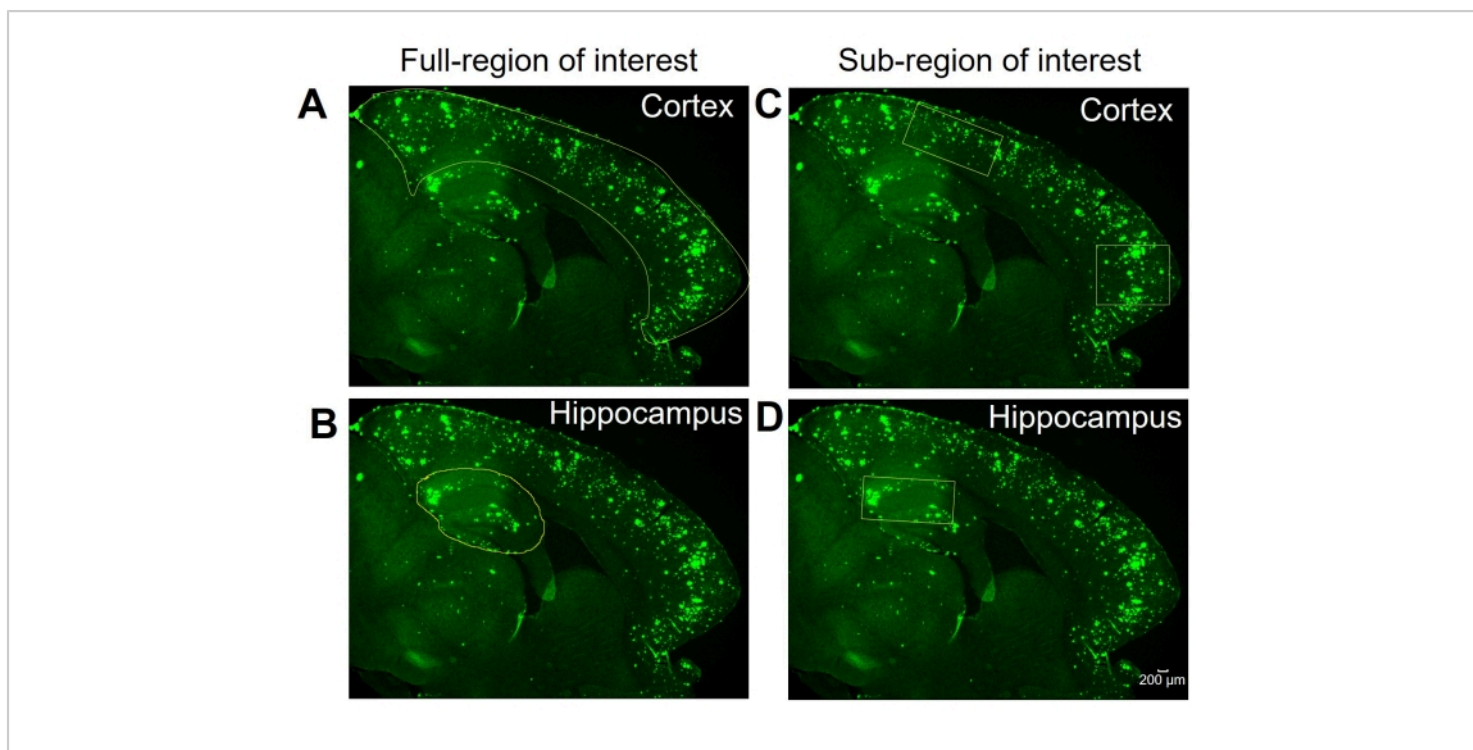


**Figure 1: Full- versus sub-regions of interest selection.** Representative images showing the full iso-cortex (cortex) and hippocampus outlined for the full-region of interest analysis in (A) and (B), respectively. Representative images show the selection of sub-region/s of the cortex and hippocampus for the sub-region of interest analysis in (C) and (D), respectively. Scale bar = 200 μm. [Please click here to view a larger version of this figure.](#)



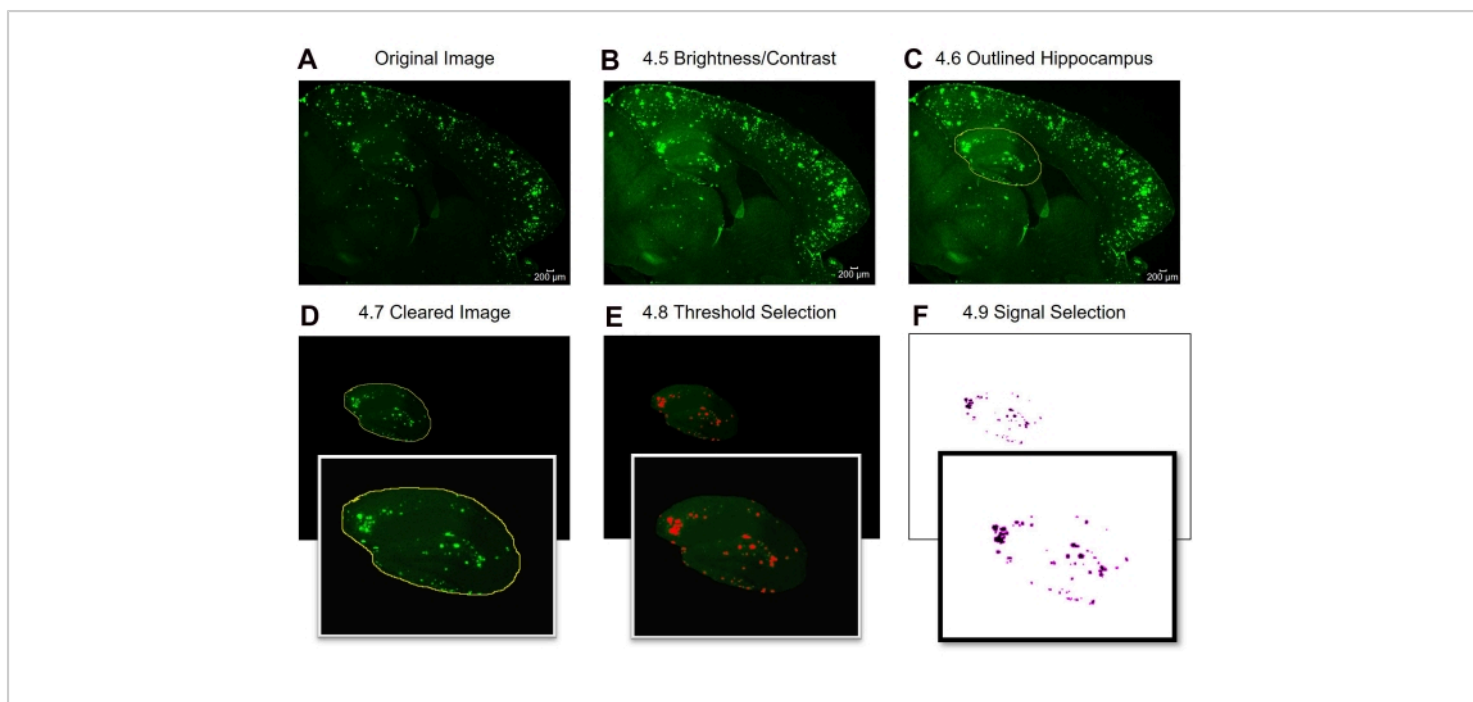


**Figure 2: Protocol for the full-region of interest 6E10-positive area quantification.** Image analysis steps showing the original image (A), the image after brightness/contrast adjustment (B), selection of the area of interest (C), clearing (D), threshold adjustment (E), and the final image ready for analysis (F). The numbers in the figure designate the step numbers in the protocol. Scale bar = 200 μm. [Please click here to view a larger version of this figure.](#)

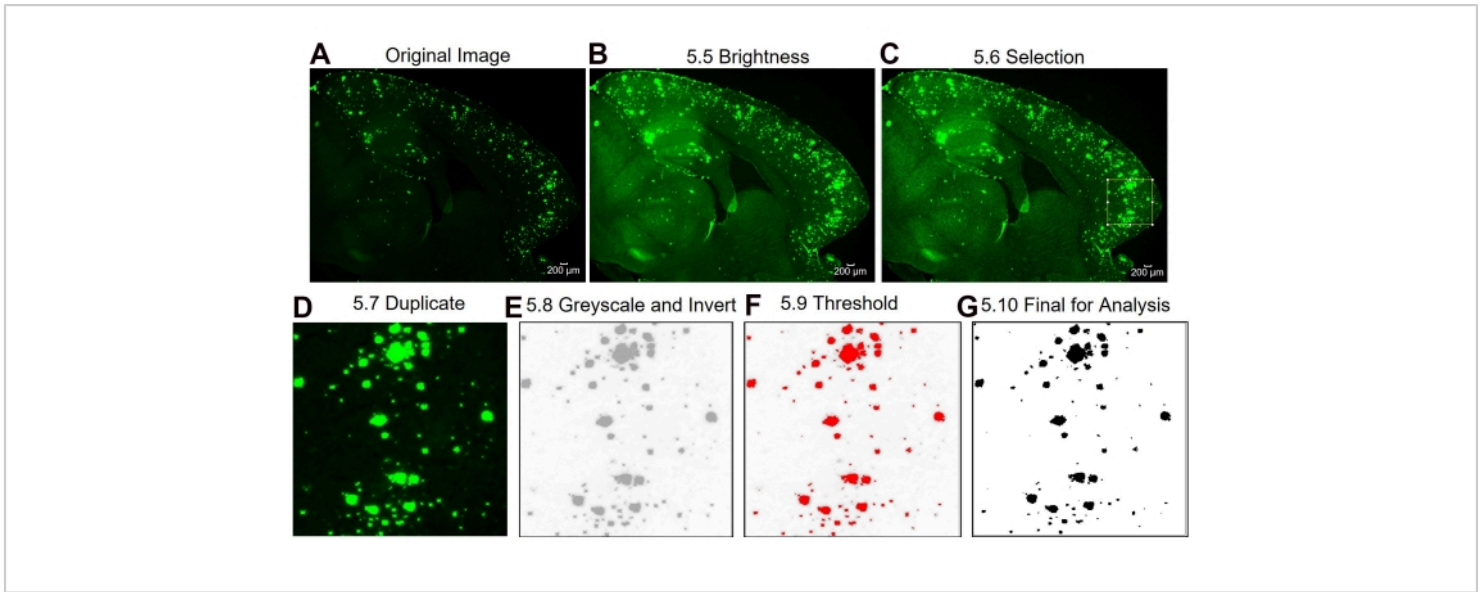


**Figure 3: Protocol for the sub-region of interest 6E10-positive area quantification.** Image analysis steps showing the original image (A), the image after brightness/contrast adjustment (B), selection of the area of interest (C), duplication of the image of the region of interest (D), changing the image to 8-Bit and inverting the image (E), threshold adjustment (F), and final image ready for analysis (G). The numbers in the figure designate the step numbers in the protocol. Scale bar = 200  $\mu\text{m}$ . [Please click here to view a larger version of this figure.](#)

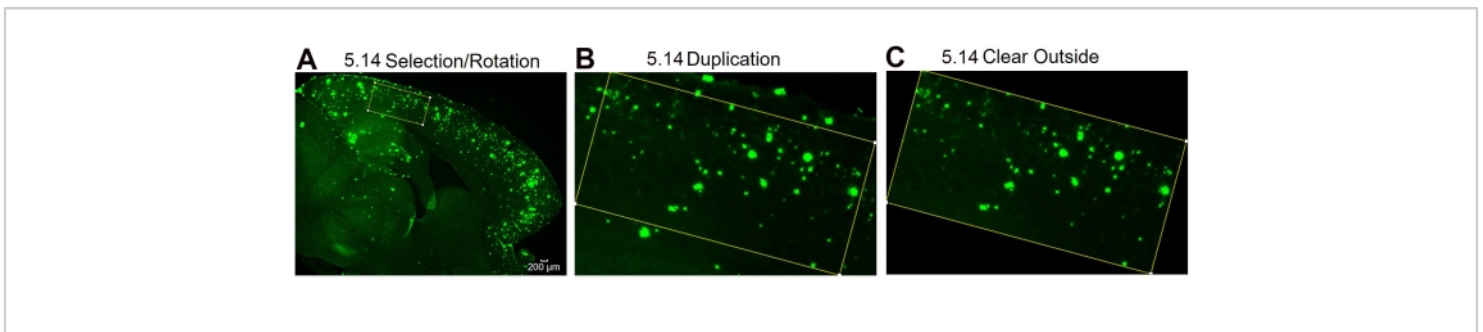


**Figure 4: Protocol for the region of interest rotation.** Image analysis steps showing the selection of the area of interest and rotation of the selection box to fit the tissue curvature (A), the image of the region of interest after duplication (B), and the image after clearing the outside (non-region of interest) area (C). The numbers in the figure designate the step number in the protocol. Scale bar = 200  $\mu\text{m}$ . [Please click here to view a larger version of this figure.](#)

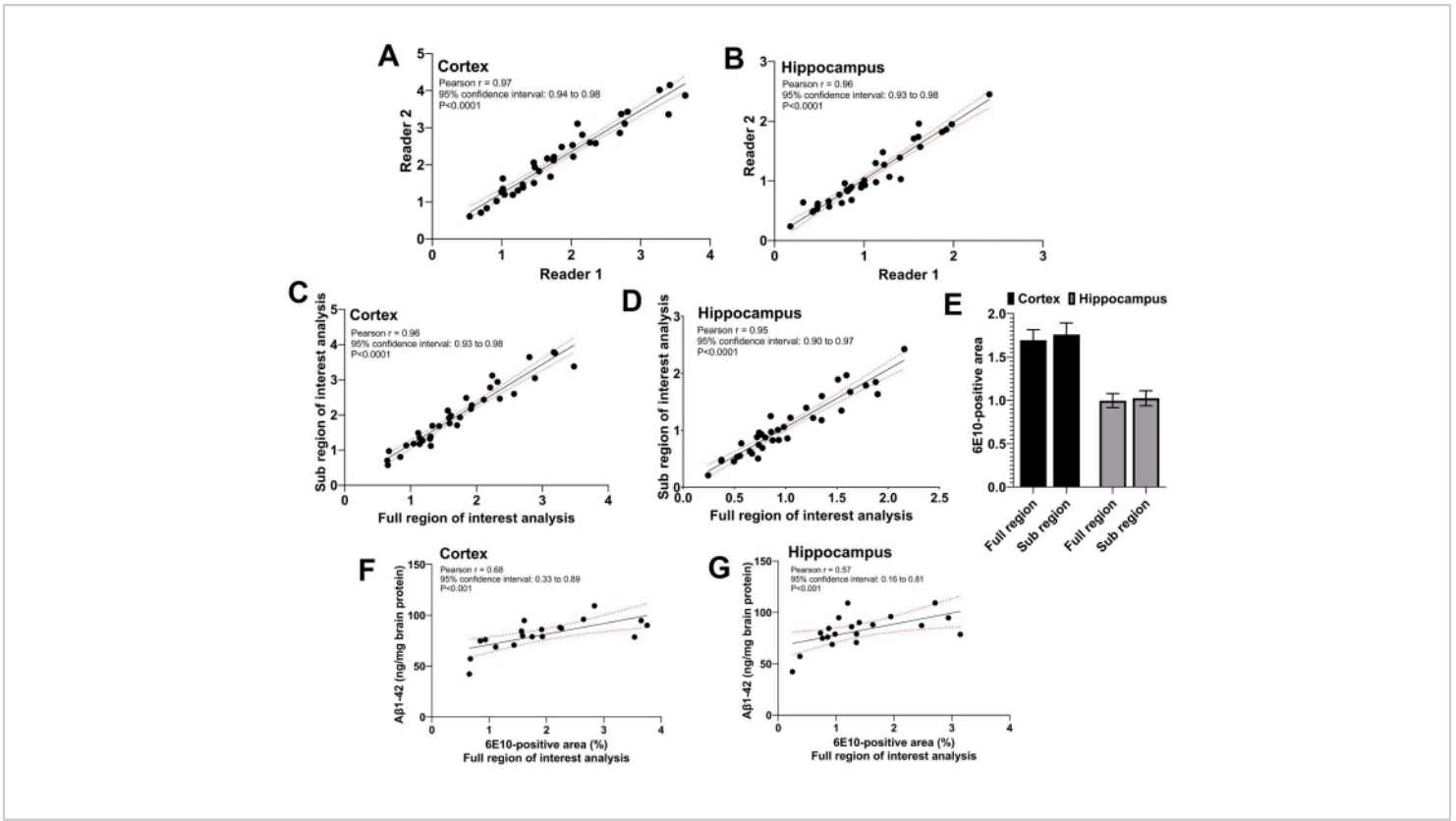


**Figure 5: Correlation between the full- and sub-regions of interest analyses.** Scatter plots show the correlation between the 6E10-positive area by the two independent readers performing the sub-region of interest analysis for the cortex (A) and the hippocampus (B). A strong positive correlation is observed between the 6E10-positive area resulting from the sub-region of interest analysis and the full-region of interest analysis for both the cortex (C) and the hippocampus (D). There is no statistically significant difference in the mean 6E10-positive area by the full-region of interest and the sub-region of interest analyses in the cortex and the hippocampus (E). A significant correlation is observed between whole-brain homogenate insoluble A $\beta$ 1-42 measurements using ELISA and the full-region of interest analysis for both the cortex (F) and the hippocampus (G). Data were analyzed using the Pearson correlation coefficient,  $r$ , in (A-D) and (F-G), and using two-way repeated-measures ANOVA in (E) using a graphing and statistics software. Data are presented as mean  $\pm$  standard error of the mean (SEM) of  $n = 35$  mice in (E), and a two-tailed  $p < 0.05$  was considered statistically significant. [Please click here to view a larger version of this figure.](#)

## Discussion

The protocol described herein outlines the procedure for hemi-brain preparation for sagittal sectioning, immunofluorescent staining of A $\beta$  deposits using the 6E10 antibody on free-floating sections, imaging of the A $\beta$ -stained

brain sections followed by quantification of the A $\beta$  deposits in the cortex and the hippocampus of mouse brain tissue using an image analysis software. While there are published protocols to quantify A $\beta$  load in brain tissue sections<sup>8,10</sup>, this protocol describes the steps involved in the quantification of

A $\beta$  load in the entire iso-cortex (referred to as cortex) and hippocampus in comparison with the A $\beta$  load in a sub-region of interest in the cortex and the hippocampus, when this may be desired. The correlation between the full- versus sub-regions of interest analyses is also provided.

There are several critical steps in the protocol. First, the protocol described is for 20  $\mu$ m thick brain tissue sections subjected to free-floating immunostaining, which results in optimal antibody penetration within the tissue section<sup>18</sup>. The free-floating technique may require the tissue sections to be manually transferred between the different solutions during the immunofluorescent staining, and careful handling of the tissue sections throughout the procedure. This is especially crucial when the tissue sections are immersed in the 70% formic acid solution for antigen retrieval in the current protocol, increasing tissue fragility for thin sections. Alternate approaches to the described protocol include using thicker tissue sections (e.g., 30-40  $\mu$ m) or using tissue sections that are directly mounted onto positively-charged slides before the immunofluorescent staining. Second, the protocol described herein uses a fluorescently-labeled 6E10 antibody. Besides using the fluorescently-labeled 6E10 antibody, non-fluorescent 6E10 antibodies (e.g., horseradish peroxidase-conjugated 6E10 antibody) can also be used to detect A $\beta$  load in brain tissue sections, and the current protocol can be adapted to quantify A $\beta$ -positive immunochemical stains in the brain tissue sections as described previously<sup>8</sup>. Third, the accuracy of the results for A $\beta$  load quantification will depend on the appropriate threshold selection in the analysis software, which is dependent on the tissue background and signal intensity. Threshold selection must be performed by the end-user such that only A $\beta$ -positive stains are selected for quantification. End-user intervention is required to optimize the specific threshold that can be applied to all

the images to assure the accuracy of the threshold setting. Fourth, since the sub-region of interest analysis requires selecting a small region of interest in the tissue section, two independent readers were used for this analysis. To maintain independence and blinding during data collection, all the images were number coded; the image analysis sequence was randomized between the readers such that the different readers analyzed different images at any given time, and the data was submitted at the end of each week. Due to the increased likelihood of inter-reader variability in the region of interest selection in the sub-region of interest analysis, the readers were trained using several sample images to optimize region selection in the cortex and the hippocampus before beginning the data collection. This training is crucial to reduce inter-reader variability, and as can be seen (**Figure 5A,B**), the 6E10-positive area reported by both the readers shows a strong relative agreement in the current study.

The current protocol and the results provide valuable information about the impact of the region of interest size on A $\beta$ -positive area quantification. A larger region of interest is expected to represent the tissue more than a smaller region of interest. Therefore, sampling a larger tissue is desirable to accurately quantify the A $\beta$  load in tissues. However, in the case of homogenous A $\beta$  load distribution within the tissue, a smaller sampling region is generally considered a good representation of the larger tissue under analysis. The current study results confirm this, and the A $\beta$  load in the entire cortex and the hippocampus was a strong correlate of A $\beta$  load in a selected sub-region of the cortex and the hippocampus (**Figure 5C,D**). To further confirm the agreement between the full- and sub-regions of interest analyses, the mean 6E10-positive area in the cortex and the hippocampus were compared, and no difference between the two methods (**Figure 5E**) was found. This confirms that either of these

methods (full- or sub-region analysis) yield comparable A $\beta$  load measurements.

The current protocol has some limitations. The two methods (full-region versus sub-region analysis) may not always be used interchangeably. The choice of using the full- or sub-region analysis will depend on the regional distribution of A $\beta$  within the tissue, which is impacted by the age, sex, and strain of the AD mouse model. At 13 months, the A $\beta$  load is distributed throughout the cortex and hippocampus of the APP/PS1 mice. However, at 6 months, A $\beta$  deposits are limited to the cortex, and minimal deposits are observed in the hippocampus<sup>12</sup>. Under such conditions, the full-region of interest analysis may be the desired approach to increase the tissue sampling area and thereby the A $\beta$  signal. On the other hand, sub-region analysis may be the method of choice when A $\beta$  load in a specific brain region is of interest, (e.g., the somatosensory cortex). Additionally, at 13 months, the APP/PS1 male mice demonstrate intense 6E10-positive stains, and the immunofluorescent staining results in an excellent signal with a very low background, making the current protocol very suitable for quantification under the given conditions. It is unclear if this quantification method can be applied successfully to less intense staining, and future work will be required to answer this question. The immunofluorescent and image quantification method presented herein detects all forms of A $\beta$ , including the precursor form<sup>13</sup>. As a result, if there is an interest in the detection of a specific A $\beta$  specie (e.g., A $\beta$ 1-40 or A $\beta$ 1-42), antibodies specific to these A $\beta$  isoforms can be used. Therefore, though the 6E10 immunofluorescent staining and detection method correlated with the measurements of A $\beta$ 1-42 measurements in whole-brain homogenates using ELISA (**Figure 5F,G**), the correlation was only modest. This can be attributed to the measurement of only A $\beta$ 1-42 using

the ELISA and detection of all A $\beta$  species using the 6E10 immunostaining. The current study uses three readers to assess the agreement and correlation between the full- and sub-regional analyses. Having additional readers may improve the robustness of the study and can further validate the agreements between the two methods presented here. Further, we use the Pearson correlation as a measure of agreement, which is widely used among other methods to describe the agreement between continuous variables<sup>19</sup>. However, one limitation of using the Pearson correlation to determine agreement is that the two methods used herein may provide related results, but one method may result in overall higher values than the other due to systematic bias. Therefore, Pearson correlation is a good measure of relative agreement<sup>19</sup>. To increase the robustness of the protocol, additional methods to confirm the absolute agreement, such as comparing the mean 6E10-positive area by the two methods (**Figure 5E**), can be used<sup>19</sup>. Taken together, the current protocol compares the A $\beta$  load detected by immunofluorescent staining and analyzes the full- and sub-regions of interest in brain tissue sections. The results show a strong correlation between these two methods for brain tissue sections derived from 13-month-old APP/PS1 male mice that show abundant A $\beta$  deposits.

## Disclosures

The authors have nothing to disclose.

## Acknowledgments

Research reported in this publication was supported by the National Institute of Aging of the National Institutes of Health under award numbers R01AG062840 (to RKS) and R01AG072896 (to RKS). The content is solely the authors' responsibility and does not necessarily represent the official

views of the National Institutes of Health. Approximately \$200k (100%) of federal funds supported this project. We would also like to thank Dr. Joshua Yang for his assistance with manuscript editing.

## References

1. Alzheimer's Association. 2021 Alzheimer's disease facts and figures. *Alzheimer's & Dementia*. **17** (3), 327-406 (2021).
2. Langa, K. M., Foster, N. L., Larson, E. B. Mixed dementia: emerging concepts and therapeutic implications. *Journal of the American Medical Association*. **292** (23), 2901-2908 (2004).
3. Gandy, S., DeKosky, S. T. Toward the treatment and prevention of Alzheimer's disease: rational strategies and recent progress. *Annual Review of Medicine*. **64**, 367-383 (2013).
4. Bloom, G. S. Amyloid-beta and tau: the trigger and bullet in Alzheimer disease pathogenesis. *JAMA Neurology*. **71** (4), 505-508 (2014).
5. Gremer, L. *et al.* Fibril structure of amyloid-beta(1-42) by cryo-electron microscopy. *Science*. **358** (6359), 116-119 (2017).
6. Ferrero, J. *et al.* First-in-human, double-blind, placebo-controlled, single-dose escalation study of aducanumab (BIIB037) in mild-to-moderate Alzheimer's disease. *Alzheimer's & Dementia Translational Research & Clinical Interventions*. **2** (3), 169-176 (2016).
7. Poon, C. H., Wang, Y., Fung, M. L., Zhang, C., Lim, L. W. Rodent models of amyloid-beta feature of Alzheimer's disease: development and potential treatment implications. *Aging and Disease*. **11** (5), 1235-1259 (2020).
8. Christensen, A., Pike, C. J. Staining and quantification of beta-amyloid pathology in transgenic mouse models of Alzheimer's disease. *Methods in Molecular Biology*. **2144**, 221 (2020).
9. Thakker, D. R. *et al.* Intracerebroventricular amyloid-beta antibodies reduce cerebral amyloid angiopathy and associated micro-hemorrhages in aged Tg2576 mice. *Proceedings of the National Academy of Sciences of the United States of America*. **106** (11), 4501-4506 (2009).
10. Song, Z. *et al.* Detecting amyloid-beta accumulation via immunofluorescent staining in a mouse model of Alzheimer's disease. *Journal of Visualized Experiments*. **170**, e62254 (2021).
11. Sun, J. *et al.* Hematologic safety of chronic brain-penetrating erythropoietin dosing in APP/PS1 mice. *Alzheimer's & Dementia Translational Research & Clinical Interventions*. **5**, 627-636 (2019).
12. Jankowsky, J. L. *et al.* Mutant presenilins specifically elevate the levels of the 42 residue beta-amyloid peptide in vivo: evidence for augmentation of a 42-specific gamma secretase. *Human Molecular Genetics*. **13** (2), 159-170 (2004).
13. Grant, M. K. O. *et al.* Human cerebrospinal fluid 6E10-immunoreactive protein species contain amyloid precursor protein fragments. *PloS One*. **14** (2), e0212815 (2019).
14. Gage, G. J., Kipke, D. R., Shain, W. Whole animal perfusion fixation for rodents. *Journal of Visualized Experiments*. **65**, e3564 (2012).
15. Eichenbaum, K. D. *et al.* Minimally invasive method for murine brain fixation. *Biotechniques*. **39** (4), 487-490 (2005).

16. Chang, R. et al. Blood-brain barrier penetrating biologic tnf-alpha inhibitor for Alzheimer's disease. *Molecular Pharmaceutics*. **14** (7), 2340-2349 (2017).
17. Pinskiy, V. et al. High-throughput method of whole-brain sectioning, using the tape-transfer technique. *PloS One*. **10** (7), e0102363 (2015).
18. Potts, E. M., Coppotelli, G., Ross, J. M. Histological-based stainings using free-floating tissue sections. *Journal of Visualized Experiments*. **162**, e61622 (2020).
19. van Stralen, K. J., Dekker, F. W., Zoccali, C., Jager, K. J. Measuring agreement, more complicated than it seems. *Nephron Clinical Practice*. **120** (3), c162-c167 (2012).